Image potential states on periodically corrugated metal surfaces

Jun Lei
Department of Physics, Shanghai Jiao Tong University, Shanghai 200030, People's Republic of China

Hong Sun*
Department of Physics, Shanghai Jiao Tong University, Shanghai 200030, People's Republic of China and Department of Physics, University of California at Berkeley, Berkeley, California 94720-7300

K. W. Yu
Department of Physics, The Chinese University of Hong Kong, Shatin, New Territories, Hong Kong

Steven G. Louie and Marvin L. Cohen
Department of Physics, University of California at Berkeley, and Material Sciences Division, Lawrence Berkeley National Laboratory, Berkeley, California 94720
(Received 12 July 2000; published 9 January 2001)

Image potential states (IPS's) on periodically stepped metal surfaces have been calculated within an impenetrable surface model. Band splittings and band anticrossings are predicted for IPS's caused by the lateral back scatterings of the stepped surfaces. A reduction in the binding energy of the lowest IPS's was found due to the lateral confinement, which agrees fairly well with the experimental results. The calculated photoionization transition-matrix elements show that the photoionization of the lowest-energy IPS's on the stepped metal surface is nearly the same as that on planar metal surfaces, while for the high-energy IPS's the umklapp process becomes important in the photoionization, giving rise to electron scattering in different directions.

DOI: 10.1103/PhysRevB.63.045408 PACS number(s): 73.20.At, 73.21.−b

I. INTRODUCTION

Image potential states (IPS's) play a significant role in many areas of surface physics. As the electrons in IPS's are bound only a few Å above the solid surface, their behavior can reveal important physical and chemical characteristics of the surface. For example, in low-energy electron diffractions, IPS's are responsible for a wealth of low-energy, fine structures attributed to surface resonances above the vacuum level.[1,2] In scanning tunneling microscope (STM) studies, it has been demonstrated that the interaction of the tunneling electrons with the dynamical image potentials of the surface and tip has profound effects on the tunneling current of the STM.[3,4] Highly spin-polarized IPS's observed in front of $Co(10\bar{1}0)$ indicate that IPS's can be employed as probes for detecting surface magnetizations.[5] Studies of the sensitive dependence of the dynamical behavior[6] and band dispersion[7,8] of the IPS's on adatoms and their patterns on the metal surfaces helped to gain deeper understandings of the adsorption process on metal surfaces. Very recently with the advent of nanostructure fabrication and high-resolution detection techniques, IPS's near nanostructured surfaces have again attracted considerable attention.[7–11] Sample fabrication via the use of atomic-scale techniques, such as vicinal surface miscut[9–11] or the addition of patterned adatoms[7] on surfaces, has created fine periodically corrugated metal surface structures with lateral periods of about 10 Å. The energy bands of IPS's on these nanostructured surfaces, measured directly using angle-resolved inverse photoemission and two-photon photoemission (2PPE), show clear evidence of localized states,[9] band folding,[10] and band splitting[7] due to the lateral confinement. However, the experimental results are diverse. Both dispersionless band[9] and backfolded dispersion band[10] of the IPS's on the stepped Cu(001) surface were reported.

Theoretical explanations of the experimental results, to our knowledge, were mainly based on simple models describing the stepped surface by a one-dimensional, Kronig-Penney potential,[10,11] although complicated numerical calculations of the IPS's on *planar* metal surfaces have been carried out.[11–15] The effects of the stepped surface on the image potential and then on the IPS's are not directly evaluated. The backfolding of the IPS bands into the first Brillouin zone (FBZ) associated with the lateral period of the stepped surface can cause band anticrossing between different IPS bands in the FBZ, since the energy of the umklapp process $\hbar^2 K_{\pm 1}^2/2m_e \approx 0.668$ eV for a lateral period of $L_x = 15$ Å is close to the energy difference (0.638 eV) between the $n=1$ and $n=2$ IPS's. In certain cases, this band anticrossing is expected to change the energy dispersions of the IPS's greatly. The umklapp process mentioned above also introduces complexity in obtaining the band structures of the IPS's with the angle-resolved 2PPE, where the direction of the photoionized electrons is detected to determine the in-plane wave vector k_x of the IPS's.[16] It is important to know in what cases electron transitions to the continuum states with in-plane wave vectors $k_x - K_m$ will dominate the photoionization, where K_m is the reciprocal-lattice wave vector associated with the stepped surface. In this paper, we present calculations of the IPS's near periodically stepped metal surfaces aimed at analyzing the problems mentioned above. Simple impenetrable metal surfaces are assumed in the calculation, which enabled us to evaluate directly the effect of the stepped surface on the image potential and IPS's. For

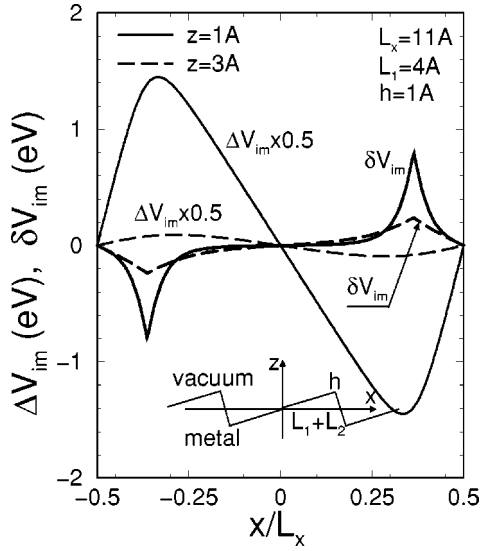

FIG. 1. $\Delta V_{im}(\mathbf{r})$ and $\delta V_{im}(\tilde{\mathbf{r}})$ (defined in the text) plotted as functions of x (or $\tilde{x}$) with z (or $\tilde{z}$) being fixed at (a) z (or $\tilde{z}$) $=1$ Å and (b) z (or $\tilde{z}$) $=3$ Å for a periodically stepped surface sketched in the figure. The structural parameters of the surface are $L_x=11$ Å, $L_1=4$ Å ($L_1+L_2=L_x/2$) and $h=1$ Å.

metal surfaces where the electron vacuum energy level lies close to the bulk electron energy bands,[16] the validity of the application of the impenetrable surface model may be questionable, as in this case the penetration of the wave functions of the IPS's into the metals will affect the binding energy and localization positions, etc., of the lowest ($n=1$) IPS's. But for the high-energy-level ($n\geqslant 2$) IPS's, and for metal surfaces where the electron vacuum energy level lies in the middle of a wide bulk electron energy gap,[16] such as a Cu(001) surface, which is the stepped metal surface studied in most of the experiments, the model of the impenetrable surface provides a reasonably good approximation.

II. FORMALISM

The IPS's on a periodically stepped, impenetrable metal surface are calculated with the method we developed previously in the calculation of the electronic states of corrugated lateral superlattices.[17] In the effective-mass approximation, the electronic system is described by minimizing the following functional:

$$L[\Phi]=\int\left\{\frac{\hbar^2}{2m^*}|\nabla\Phi(\mathbf{r})|^2+V_{im}(\mathbf{r})|\Phi(\mathbf{r})|^2\right\}d\mathbf{r}$$
$$-E\int|\Phi(\mathbf{r})|^2d\mathbf{r}, \tag{1}$$

where m^* is the electron effective mass. $\Phi(\mathbf{r})$ and E are the electron wave function and energy eigenvalue of the IPS to be determined. $V_{im}(\mathbf{r})$ is the electron self-induced image potential outside the stepped metal surface, which we derived previously:[18]

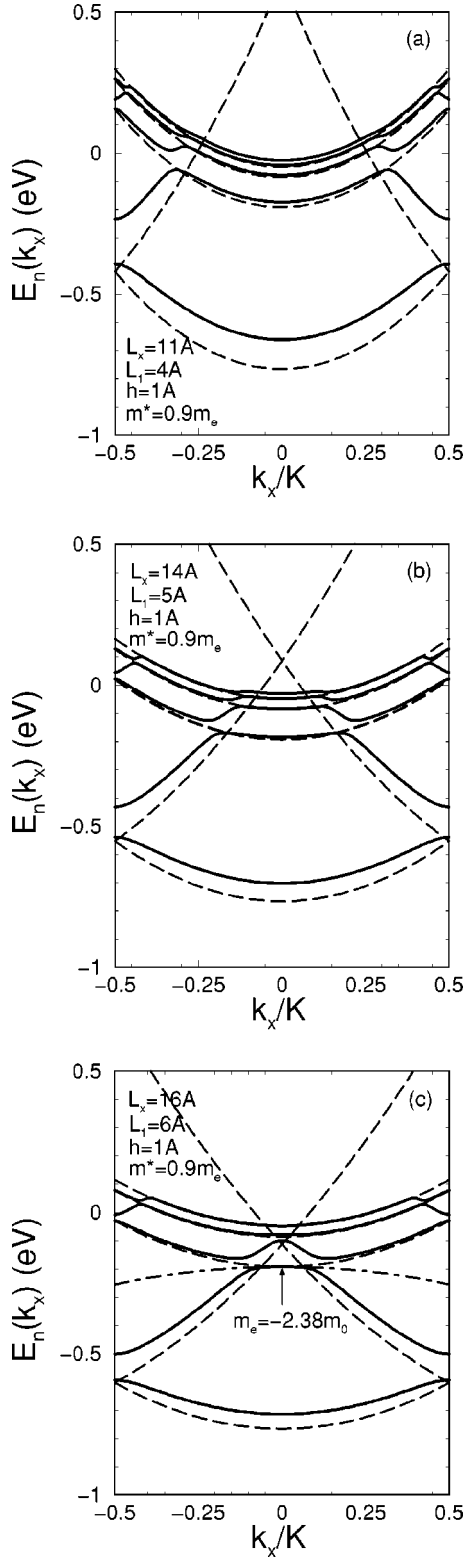

FIG. 2. The first five calculated energy bands (the solid lines) of the IPS's near the periodically stepped metal surfaces similar to those in Fig. 1, with different lateral periods, (a)–(c). An electron effective mass $m^*=0.9m_e$ is assumed. The dash-dotted line in (c) indicates the parabolic fit of the $n=2$ energy band. The energy bands (the dashed lines) for the IPS's of the planar metal surfaces are also plotted in the same figure.

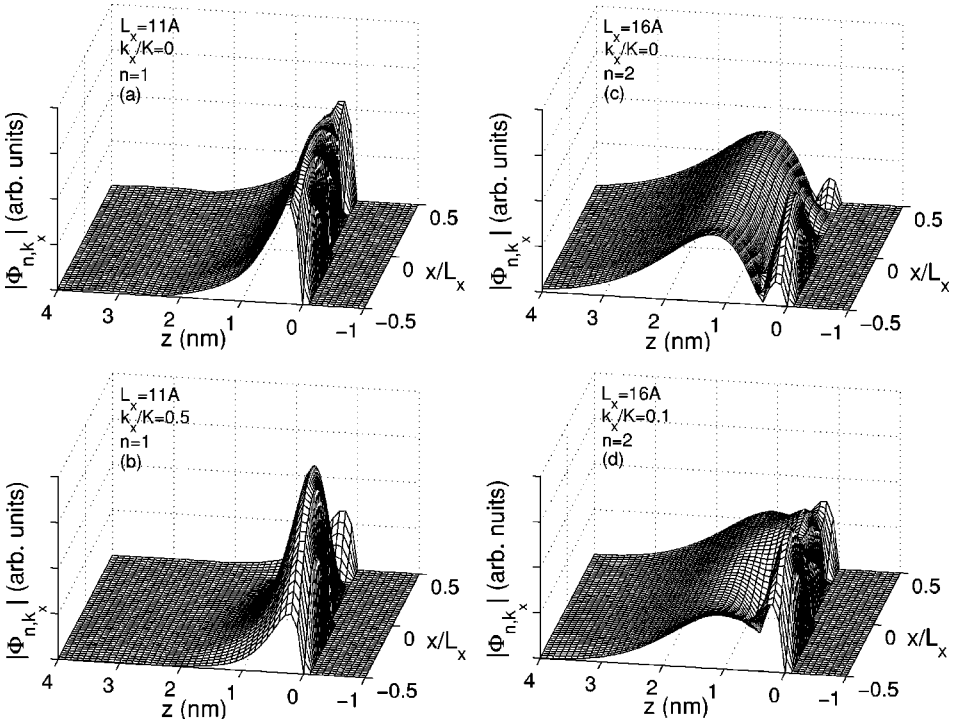

FIG. 3. The calculated wave functions of the IPS's in one period for (a,b) the lowest energy level ($n=1$) on the stepped surface of Fig. 2(a), and (c,d) the $n=2$ states on the stepped surface of Fig. 2(c). The in-plane wave vectors for the IPS wave functions are (a,c) $k_x/K=0$, (b) $k_x/K=0.5$, and (d) $k_x/K=0.1$.

$$V_{im}(\mathbf{r}) = -\frac{e^2}{4z} + \Delta V_{im}(\mathbf{r}) \tag{2}$$

with

$$\Delta V_{im}(\mathbf{r}) = -\frac{e^2}{2\pi}\int dx'dy' f(x') \times \frac{z^2}{[(y'-y)^2+(x-x')^2+z^2]^3}, \tag{3}$$

where we assume that the metal occupies the space $z<f(x)$, with its surface described by a profile function $z=f(x)$. The first term on the right-hand side of Eq. (2) is the image potential for a planar metal surface, while the second term gives the modification due to the stepped surface. To overcome the difficulty associated with the complicated boundary conditions on the stepped interface, we introduce the following coordinate transformation:

$$\tilde{x}=x; \quad \tilde{y}=y; \quad \tilde{z}=z-f(x), \tag{4}$$

which transforms the stepped surface into a plane at $\tilde{z}=0$. The electron wave function of the IPS is expanded with a complete set of eigenwave functions in the transformed space $\tilde{\mathbf{r}}$:

$$\tilde{\Phi}_{nk_x}(\tilde{\mathbf{r}}) = \sum_{n'm'} A_{n'm'}(n,k_x)\frac{e^{-i(k_x-K_{m'})\tilde{x}}}{\sqrt{L_x^{(0)}}}\zeta_{n'}(\tilde{z}), \tag{5}$$

where $\zeta_{n'}(\tilde{z})$ is the eigenwave function of the IPS on a *planar* impenetrable surface[19] in space $\tilde{\mathbf{r}}$. The in-plane wave vector k_x of the IPS is limited within the FBZ ($|k_x|\leq K/2=\pi/L_x$) and $K_{m'}=m'K$. The energy band $E_n(k_x)$ of the IPS is obtained by diagonalizing the eigenvalue equation obtained by minimizing the functional $L[\Phi]$.[17] A sufficient number of the expansion functions (n',m') are used in the calculation so that the variation of the first three calculated energy bands is less than 1% if the number of the expansion functions are further increased.

Before giving the calculated results, it is instructive to analyze the image potential of the stepped metal surface in more detail. In the transformed space $\tilde{\mathbf{r}}$, we can also divide the image potential into

$$\tilde{V}_{im}(\tilde{\mathbf{r}}) = -\frac{e^2}{4\tilde{z}} + \delta V_{im}(\tilde{\mathbf{r}}). \tag{6}$$

Both $\Delta V_{im}(\mathbf{r})$ and $\delta V_{im}(\tilde{\mathbf{r}})$ are given in Fig. 1 with z and $\tilde{z}$ fixed at (a) z (or $\tilde{z}$) $=1$ Å and (b) z (or $\tilde{z}$) $=3$ Å for the stepped Cu(001) surface similar to that reported in Ref. 10. The structural parameters of the surface (see the sketch in Fig. 1) are $L_x=11$ Å, $L_1=4$ Å ($L_1+L_2=L_x/2$) and $h=1$ Å. Both $\delta V_{im}(\tilde{\mathbf{r}})$ and $\Delta V_{im}(\mathbf{r})$ decrease quickly away from the surface. This explains why experimental results[11] show small changes for the high level IPS's which are localized far away from the stepped surfaces. But we will show that the anticrossing of the energy bands can still introduce significant changes in the energy bands of these IPS's. It is also interesting to note that the signs of $\delta V_{im}(\tilde{\mathbf{r}})$ and $\Delta V_{im}(\mathbf{r})$ are opposite. As $\tilde{z}=z-f(x)$ is the z direction distance of the electron to the surface, $\delta V_{im}(\tilde{\mathbf{r}})$ in Fig. 1 gives the lateral potential felt by the electron with its z direction distance to the surface being fixed. As the electron is bound near the metal surface by the repulsive force of the surface (impenetrable) barrier and the attractive force of the image potential with its distance to the surface being almost fixed, we will show that it is $\delta V_{im}(\tilde{\mathbf{r}})$ which determines mainly where the electron in the IPS is localized laterally on the stepped surface.

III. RESULTS AND DISCUSSION

We give in Fig. 2 the first few calculated energy bands (the solid lines) of the IPS's near the periodically stepped metal surfaces similar to that sketched in Fig. 1, with different lateral periods [Figs. 2(a)–2(c)]. An electron effective mass $m^*=0.9m_e$ is assumed in the IPS's of the Cu(001) surface.[20] Also given in Fig. 2 are the energy bands (the dashed lines) of the IPS's for the *planar* metal surface. Reductions in the binding energies of the lowest IPS's are predicted for all the stepped metal surfaces calculated. A reduction in the binding energy of the lowest IPS was observed in both the stepped Cu(001) surface[10] adsorbed with Na atoms ($\sim$0.01 ML) with a lateral period of $L_x=11$ Å and the stepped Cu(111) surface[11] with $L_x=14$ Å. The theoretical reductions in the binding energy of the IPS's that we obtained are 94 meV [Fig. 2(a)] and 63 meV [Fig. 2(b)], in fairly good agreement with the observed reduction of 120 and 50 meV, respectively. The reduction in the binding energy of IPS's has also been reported on rough Cu(111) surfaces.[21] This reduction is attributed to the lateral localization of the IPS's by the stepped metal surface. The high level IPS's are less affected by the stepped surface because these states are bound further away from the surface, as discussed in the last paragraph of Sec. II. But the band anticrossing between the high level bands and the backfolded $n'=1$ band introduce detectable changes in these high level bands. For a stepped metal surface with $L_x=16$ Å, a negative effective electron mass is predicted for the $n=2$ IPS in the center of the FBZ [Fig. 2(c)]. Experimentally, to our knowledge, no results on stepped Cu metal surface with $L_x\geqslant 16$ Å were reported. While the $n=2$ IPS band for a stepped Cu(111) surface[11] with $L_x=14$ Å was measured within $|k_x|<0.1$ Å^{-1} (or $|k_x/K|<0.22$), just before the band anticrossing effect is expected to appear [see Fig. 2(b)]. The band splitting of the IPS's at the edge of the FBZ were reported for the Co($10\bar{1}0$) surface[5] and the Si(111) surface[7] adsorbed with 4×1 patterned In atoms. While on the stepped Cu(001) surface,[10] only the lower level of the splitting bands at the edge of the FBZ was observed.

In Figs. 3(a) and 3(b), we plot in one period the wave functions of the IPS's of the lowest energy level ($n=1$) on the stepped surface of Fig. 2(a), and in Figs. 3(c) and 3(d), the $n=2$ states on the stepped surface of Fig. 2(c). The in-plane wave vectors for the IPS wave functions are $k_x/K=0$, $k_x/K=0.5$, and $k_x/K=0.1$ in Figs. 3(a), 3(c), 3(b), and 3(d), respectively. The electrons in the $n=1$ IPS's [Figs. 3(a) and 3(b)] localize laterally at the bottom of the steps, where $\delta V_{im}(\vec{\mathbf{r}})$ shows a potential valley (see Fig. 1) as we expected. Vertically, the electrons in the $n=1$ IPS's are bound at about $\sim$3 Å above the stepped surface. While for the $n=2$ IPS's, electrons are bound further away at about $\sim$12 Å from the surface, which reduces the effect of the stepped surface on these states. But at the band anticrossing, there is a strong mixture of the wave functions from different bands [Fig. 3(d)].

This mixture of wave functions complicates the analysis of the experimental results from angle-resolved 2PPE, as the electrons in the photoionization process can make the transition to different continuum states with in-plane wave vectors at k_x-K_m, giving rise to electrons with the same kinetic energy, but scattering in different directions. To analyze the transition strength of the photoionization, we calculate the photoionization transition-matrix element from the bound to continuum IPS's:

$$P_z(n,k_x-K_m)=\langle\Phi_{k_x-K_m,k_z}(\mathbf{r})|p_z|\Phi_{nk_x}(\mathbf{r})\rangle, \qquad (7)$$

where $\Phi_{k_x-K_m,k_z}(\mathbf{r})$ is the wave function of the IPS's in the continuum[19] with a kinetic energy $E_K=\hbar^2[(k_x-K_m)^2+k_z^2]/2m_e$. $P_z(n,k_x-K_m)$ is displayed in Fig. 4(a) for the stepped surfaces of Fig. 2(a), and in Fig. 4(b) for that of Fig. 2(c) as functions of k_x with a given incident photon energy $\hbar\omega=E_K-E_n(k_x)=2.2$ eV for $n=1,2$, and $m=0,\pm1$, where P_0 is the photoionization transition-matrix element on a pla-

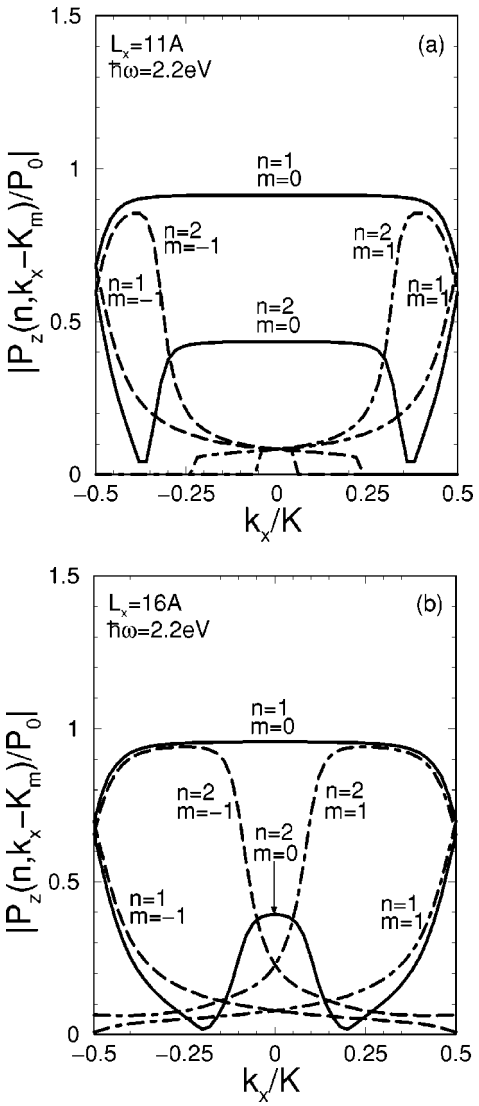

FIG. 4. The calculated photoionization transition-matrix element $P_z(n,k_x-K_m)$, (a) for the stepped surfaces of Fig. 2(a), and (b) for that of Fig. 2(c), plotted as functions of k_x with a given incident photon energy $\hbar\omega=2.2$ eV for $n=1,2$ and $m=0,\pm1$. P_0 is the photoionization transition-matrix element on a planar metal surface from the $n=1$ IPS at $k_x=0$ with the same photon energy.

nar metal surface from the $n=1$ IPS at $k_x=0$ with the same photon energy. The results in Fig. 4 show that the photoionization of the $n=1$ IPS's on the stepped surfaces is nearly the same as that on a planar surface. The umklapp processes ($m=\pm 1$) do not affect the photoionization very much, except at the boundary of the FBZ. While for the $n=2$ IPS's, the umklapp processes ($m=\pm 1$) become important in the photoionization when the energy band anticrossing starts. But in the center of the FBZ ($k_x \approx 0$), photoionization with the small angle off the surface normal ($m=0$) is the main scattering process. The negative effective mass due to the band anticrossing effect we predicted in Fig. 2(c) is expected to be detectable with angle-resolved 2PPE, because it appears at the center of the FBZ and experimentally the $n=2$ band of the IPS is observed only near the center of the FBZ.[10,11]

IV. CONCLUSION

The IPS's on periodically stepped metal surfaces have been calculated within an impenetrable surface model. Band splittings and band anticrossings are predicted for the IPS's caused by the lateral back scatterings of the stepped surfaces. Detectable effects in the energy dispersions of the IPS bands are expected. A reduction in the binding energy of the lowest IPS's was found due to the lateral confinement, which agrees fairly well with the experimental results. The calculated photoionization transition-matrix elements show that the photoionization of the lowest IPS's on the stepped metal surface is nearly the same as that on planar metal surfaces, while for the high-energy IPS's, the umklapp process becomes important in the photoionization, giving rise to electron scattering in different directions.

ACKNOWLEDGMENTS

H.S. acknowledges the financial support from the Berkeley Scholar Program funded by a generous contribution from the Tang Family Foundation. This work was also supported by the Research Fund for the Doctoral Program of Higher Education of China, the Climbing (Pan-Deng) Program of the Chinese National Committee of Science. The Direct Grant for Research at the Chinese University of Hong Kong was supported by Project No. 2060175. The research at Berkeley was supported by the Director, Office of Energy Research, Office of Basic Energy Sciences, U.S. Department of Energy, under Contract No. DE-AC03-76SF00098 and National Science Foundation Grant No. DMR-9520554.

*Corresponding author. Email address: (p) hong_sun@online.sh.cn; (t) hsun@civet.berkeley.edu

[1] E. G. McRae, Rev. Mod. Phys. **51**, 541 (1979).
[2] R. E. Dietz, E. G. McRae, and R. L. Campbell, Phys. Rev. Lett. **45**, 1280 (1980).
[3] R. Berndt, J. K. Gimzewski, and P. Johansson, Phys. Rev. Lett. **67**, 3796 (1991).
[4] M. Šunjić and L. Marušić, Phys. Rev. B **44**, 9092 (1991).
[5] S. Bode, K. Starke, P. Rech, and G. Kaindl, Phys. Rev. Lett. **72**, 1072 (1994).
[6] W. Berthold, U. Höfer, P. Feulner, and D. Menzel, Chem. Phys. **251**, 123 (2000).
[7] I. G. Hill and A. B. McLean, Phys. Rev. Lett. **82**, 2155 (1999).
[8] R. L. Lingle, Jr., D. F. Padowitz, R. E. Jordan, J. D. McNeill, and C. B. Harris, Phys. Rev. Lett. **72**, 2243 (1994).
[9] J. E. Ortega, F. J. Himpsel, R. Haight, and D. R. Peale, Phys. Rev. B **49**, 13 859 (1994).
[10] X. Y. Wang, X. J. Shen, R. M. Osgood, Jr., R. Haight, and F. J. Himpsel, Phys. Rev. B **53**, 15 738 (1996).
[11] X. Y. Wang, X. J. Shen, and R. M. Osgood, Jr., Phys. Rev. B **56**, 7665 (1997).
[12] N. V. Smith, Phys. Rev. B **32**, 3549 (1985).
[13] E. V. Chulkov, I. Sarría, V. M. Silkin, J. M. Pitarke, and P. M. Echenique, Phys. Rev. Lett. **80**, 4947 (1998).
[14] V. M. Silkin, E. V. Chulkov, and P. M. Echenique, Phys. Rev. B **60**, 7820 (1999).
[15] T. Mii and H. Ueba, J. Lumin. **87–89**, 898 (2000).
[16] R. M. Osgood, Jr. and X. Y. Wang, in *Solid State Physics: Advances in Research and Applications*, edited by H. Ehrenreich and F. Spaeper (Academic, New York, 1998), Vol. 51, p. 1.
[17] H. Sun, J. M. Huang, and K. W. Yu, J. Phys.: Condens. Matter **8**, 7605 (1996).
[18] H. Sun and S. W. Gu, Phys. Rev. B **41**, 3145 (1990).
[19] R. Shakeshaft and L. Spruch, Phys. Rev. A **31**, 1535 (1985).
[20] K. Giesen, F. Hage, F. J. Himpsel, H. J. Riess, W. Steinmann, and N. V. Smith, Phys. Rev. B **35**, 975 (1987).
[21] F. Theilmann, R. Matzdorf, and A. Goldmann, Surf. Sci. **420**, 33 (1999).